



## Moroccan speleothem and tree ring records suggest a variable positive state of the North Atlantic Oscillation during the Medieval Warm Period



J.A. Wassenburg<sup>a,\*</sup>, A. Immenhauser<sup>a</sup>, D.K. Richter<sup>a</sup>, A. Niedermayr<sup>a</sup>, S. Riechelmann<sup>a</sup>, J. Fietzke<sup>b</sup>, D. Scholz<sup>c</sup>, K.P. Jochum<sup>d</sup>, J. Fohlmeister<sup>e,f</sup>, A. Schröder-Ritzrau<sup>f</sup>, A. Sabaoui<sup>g</sup>, D.F.C. Riechelmann<sup>h</sup>, L. Schneider<sup>h</sup>, J. Esper<sup>h</sup>

<sup>a</sup> Institute of Geology, Mineralogy, and Geophysics, Ruhr University Bochum, Universitätsstrasse 150, 44801 Bochum, Germany

<sup>b</sup> GEOMAR Helmholtz Center for Ocean Research Kiel, Germany

<sup>c</sup> Institute for Geosciences, Johannes Gutenberg University, Mainz, Germany

<sup>d</sup> Biogeochemistry division, Max Planck Institute for Chemistry, Mainz, Germany

<sup>e</sup> Institute for Environmental Physics, University of Heidelberg, Heidelberg, Germany

<sup>f</sup> Heidelberg Academy of Sciences, Heidelberg, Germany

<sup>g</sup> Faculty of Sciences Dhar Mahraz, Fès, Morocco

<sup>h</sup> Department of Geography, Johannes Gutenberg University, 55099 Mainz, Germany

### ARTICLE INFO

#### Article history:

Received 31 July 2012

Received in revised form

10 May 2013

Accepted 28 May 2013

Editor: G. Henderson

Available online 10 July 2013

#### Keywords:

North Atlantic Oscillation

medieval climate anomaly

speleothem

prior calcite precipitation

aragonite

trace elements

### ABSTRACT

We present a magnesium (Mg) and strontium (Sr) record from an aragonitic speleothem (Grotte de Piste, Morocco, 34°N; 04°W) providing a reconstruction of effective rainfall from 619 to 1962 AD. The corresponding drip site was monitored over 2 yr for drip water Mg/Ca and Sr/Ca ratios. Results show evidence for prior aragonite precipitation, which can explain negative correlations between speleothem Mg and Sr concentrations. The data shown here have important climate implications concerning the evolution of the North Atlantic Oscillation (NAO). A comparison of the stalagmite data from Grotte de Piste with an updated tree ring based drought reconstruction from Morocco and other NAO related proxy records confirms that the Medieval Warm Period (MWP) was dominated by NAO+ conditions. The stalagmite record and multiple proxy records from the Iberian Peninsula, however, suggest that considerable rainfall variability occurred during the MWP. This implies that the NAO has been more variable during the MWP than formerly suggested.

© 2013 Elsevier B.V. All rights reserved.

### 1. Introduction

The North Atlantic Oscillation (NAO) represents the dominating atmospheric pressure mode of the North Atlantic/European area (Hurrell, 1995; Wanner et al., 2001) and has a large effect on winter surface air temperatures and precipitation in the Northern hemisphere (Hurrell, 1996; Hurrell and Van Loon, 1997). The NAO affects the strength and the course of the westerlies and can be described by the NAO-index, which is defined as the difference in normalized sea level pressure between the Icelandic low and the Azores subtropical high. In order to gain understanding of its natural variability, proxy based NAO reconstructions over the last hundreds to thousands of years are a necessity (Cook et al., 2002; Luterbacher et al., 1999; Olsen et al., 2012; Trouet et al., 2009). Trouet et al.

(2009) suggested that the Medieval Warm Period was characterized by persistent NAO+ conditions, whereas the Little Ice Age (LIA) was characterized by dominantly NAO- conditions. Lehner et al. (2012), however, demonstrated that the persistence of NAO+ during the MWP and the MWP-LIA transition could not be reproduced by the climate models. The NAO reconstruction from Trouet et al. (2009) thus needs to be verified by other proxy records.

The NAO reconstruction from Trouet et al. (2009) is based on a rainfall sensitive speleothem record from NW Scotland (Proctor et al., 2000) and a tree ring based PDSI reconstruction from Morocco (Esper et al., 2007). Here, trace element compositions of an aragonitic speleothem from the north-western part of the Middle Atlas in Morocco have been investigated. The speleothem record covers the time period 619–1962 AD and is from a cave located in an area sensitive to droughts, which is affected by the NAO. This is evident from the strong decrease in the amount of winter rainfall after the 1970s, which was linked to predominantly positive NAO conditions (Ward et al., 1999).

\* Corresponding author. Tel.: +49 2343227768; fax: +49 2343214201.  
E-mail address: [jasper.wassenburg@rub.de](mailto:jasper.wassenburg@rub.de) (J.A. Wassenburg).

Speleothems are well established archives of continental paleoclimate (Cruz et al., 2005; Drysdale et al., 2009; Kanner et al., 2012; Wang et al., 2008; Zhang et al., 2008). To date, most studies rely on calcitic stalagmites and flowstones (Cai et al., 2010; Neff et al., 2001; Spötl et al., 2002; White, 2004). In this study, however, an aragonitic stalagmite has been used.

Aragonite speleothems are common in dolomite host rock caves and in (seasonally) arid settings (Bertaux et al., 2002; Frisia et al., 2002; Railsback et al., 1994; Wassenburg et al., 2012). In general, aragonite is diagenetically less stable under atmospheric conditions compared to calcite and may therefore recrystallize to calcite (Frisia et al., 2002; Martin-Garcia et al., 2009). However, well preserved aragonitic speleothems provide excellent archives for climate reconstruction (Cosford et al., 2008; Li et al., 2011), because they are – due to their often high U content – well suited for U–Th dating. Whereas most studies of aragonite speleothems have focussed on oxygen isotopes (Cosford et al., 2008; Holmgren et al., 1999; Holzkämper et al., 2009; Li et al., 2011 and others), trace element compositions remain largely unexplored (Finch et al., 2003; 2001; McMillan et al., 2005; Wassenburg et al., 2012). Therefore, understanding the processes affecting speleothem aragonite trace element abundances is a necessity in order to explore their full potential.

In calcitic speleothems, positive correlations between Mg and Sr have repeatedly been interpreted in terms of prior calcite precipitation (PCP). Prior calcite precipitation (Fairchild et al., 2000; Fairchild and Treble, 2009; McMillan et al., 2005; Sherwin and Baldini, 2011; Sinclair et al., 2012; Stoll et al., 2012; Wong et al., 2011) takes place if the water encounters a gas phase with a lower  $p\text{CO}_2$  causing  $\text{CO}_2$  degassing within the karst aquifer or at the cave ceiling. This leads to super-saturation of the water with respect to  $\text{CaCO}_3$ , and precipitation (Fairchild and Treble, 2009). Under dry climate conditions, PCP can increase because of the increasing abundance of gas-filled voids within the karst aquifer

and decreasing drip rates. Nevertheless, changes in soil  $\text{CO}_2$  production and cave air  $p\text{CO}_2$  may be important as well (Sherwin and Baldini, 2011; Wong et al., 2011).

The interpretation of trace element records from aragonite speleothems differs from calcite speleothems due to (1) crystallographic differences (orthorhombic versus trigonal), (2) the possible presence of secondary calcite (Frisia et al., 2002; Martin-Garcia et al., 2009; Ortega et al., 2005), or (3) co-precipitation of both mineralogies (Holzkämper et al., 2009; Wassenburg et al., 2012). Crystallographic parameters (i.e. the space available for the cation within the crystal lattice) affect the absolute partitioning coefficients of trace elements. Therefore, PCP has a different effect on drip water trace element to Ca ratios compared to prior aragonite precipitation (PAP; Wassenburg et al., 2012).

The aims of this study are (1) to present and interpret an aragonite speleothem trace element record from the Middle Atlas in Morocco, supported by cave monitoring data; (2) to compare the speleothem record to an updated version of the tree-ring based PDSI reconstruction from Esper et al. (2007); (3) to assess the existence of the MWP-LIA transition in terms of NAO conditions and (4) to assess the persistence of NAO+ conditions during the MWP.

## 2. Case setting

### 2.1. Present day climate of the Middle Atlas

Morocco is bordered by the North Atlantic to the west, the Mediterranean Sea to the north-east and the Western Sahara to the south-east (Fig. 1). The cave investigated here is referred to as Grotte de Piste and is located in the north-western part of the Middle Atlas of Morocco (Fig. 1). According to Knippertz et al.

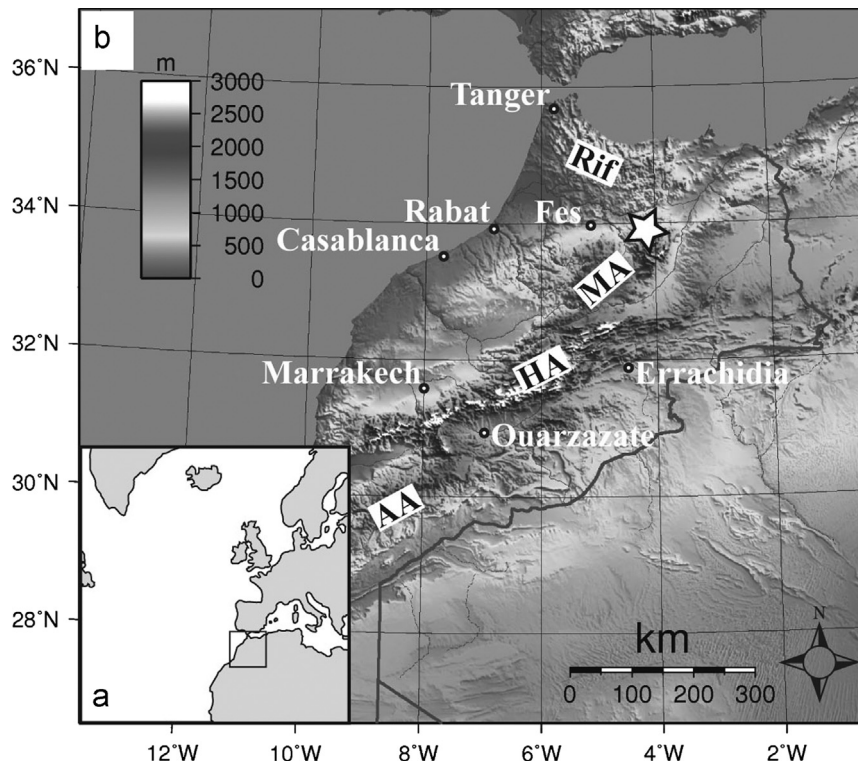


**Fig. 1.** (a) Regional setting of Morocco at the boundary between North Atlantic and Mediterranean Sea. (b) Cave position (indicated by the white star), with respect to the Rif, the Middle Atlas (MA), the High Atlas (HA), and the Anti Atlas (AA) mountain belts.

(2003), this region falls within the Atlantic climate domain. The climate of the Middle Atlas is characterized by very dry summers (< 2% of mean annual rainfall) and relatively wet winters (> 40% of mean annual rainfall). Annual precipitation measured in Bab Bou Idir (1500 m asl) near Grotte de Piste, is 862 ( $\pm$  506) mm (years defined according to the October–September rain season, 1999–2010 period).

Rainfall patterns are related to the strength and position of the Azores subtropical high, and are therefore related to the NAO index (Hurrell, 1995). During NAO– conditions, the meridional pressure gradient is relatively low, weakening the westerlies and shifting them southward (Wanner et al., 2001). Negative (positive) NAO conditions induce wetter (drier) conditions in Morocco and the Iberian Peninsula, whereas in (north) Western Europe, relatively cold (warm) and dry (wet) conditions prevail. The 2009–2010 winter season was characterized by the most extreme and persistent negative NAO conditions ever recorded (Osborn, 2011). This can be clearly recognized as a very wet winter at Bab Bou Idir (Fig. S1).

## 2.2. Cave setting

Speleothem GP5 was collected from Grotte de Piste (Fig. S2) situated in dolomitic host rock with spatially limited limestone intervals (Wassenburg et al., 2012). Grotte de Piste is located at an altitude of 1260 m above sea level. The vegetation above the cave consists of small oak trees, shrubs and grasses. About 60% of the dolomite host rock surface is covered by clay-rich soil with a thickness of up to 20 cm. Due to the cave's position close to the top of a crest; the drip water is of local origin. The cave's entrance is about 3 m wide and is characterized by a steep slope. Grotte de Piste has a lower and an upper level located approximately 20 m above the cave floor (Fig. S2). The upper level has approximately 35–40 m of overburden.

## 3. Material and methods

Stalagmite GP5, fed by a 27 cm long stalactite, has a total length of 78 cm and grew at the upper cave level at a distance of 50 m

from the entrance (Fig. S2). Here, data from the upper 20 cm of the stalagmite are presented (Fig. 2). The lower part will be the focus of another study. GP5 is partly characterized by mm scale layering made up by alternating porous and less porous layers (Fig. 2). The mineralogy of GP5 was determined by X-ray diffraction analysis (XRD; Miao et al., 2009) of hand drilled samples (ca. 20 mg). Ten percent of quartz was added to the sample powder as a standard in order to derive offsets in the {104} calcite peaks and estimate the Mg content within the crystal lattice in mol% (Füchtbauer and Richter, 1988). Samples were homogenized in an agate mortar before being analyzed. Thin section petrography was used to examine the aragonite fabric for potential diagenetic features.

Cave monitoring of Grotte de Piste was performed between March 2010 and March 2012 with samples taken in spring, summer, fall and winter. Stalagmite GP5's drip site (Fig. S2) was monitored for drip rate and drip water Mg, Sr and Ca concentrations. Drip water trace element to Ca ratios are always expressed in molar ratios. Cave air CO<sub>2</sub> concentrations were measured every fieldtrip at several positions of the cave in order to deduce information on cave air circulation (Fig. S2; Bourges et al., 2006; Frisia et al., 2011; Kowalczyk and Froelich, 2010). Cave air temperature was measured every twelve hours using permanently installed temperature loggers (I-Buttons). More details are given in the Supplement.

Eight samples of GP5 (Fig. 2) were dated using the U–Th method, which were analyzed with an AXIOM MIC-ICP-MS (Fietzke et al., 2005) at the GEOMAR Helmholtz Center for Ocean Research Kiel, Germany. Additional dating was performed with the radiocarbon method in order to find the mid 20th century atmospheric <sup>14</sup>C anomaly (“bomb-peak”) to document recent growth of the stalagmite (Fig. 2; Fohlmeister et al., 2012; Genty and Massault, 1999; Hodge et al., 2011; Matthey et al., 2008). See Supplement for details. The age-depth model was calculated using the StalAge algorithm of Scholz and Hoffmann (2011), which gives 95%-confidence limits for the age model. Additional uncertainty exists due to the thickness of the sample hole (i.e., 2.5–4 mm), this is included in the error bar.

A Thermo Finnigan Element 2 ICP-MS coupled to a New Wave UP213 laser at the Max Planck Institute for Chemistry, Mainz, Germany performed the analyses of <sup>25</sup>Mg, <sup>86</sup>Sr and <sup>43</sup>Ca. The latter

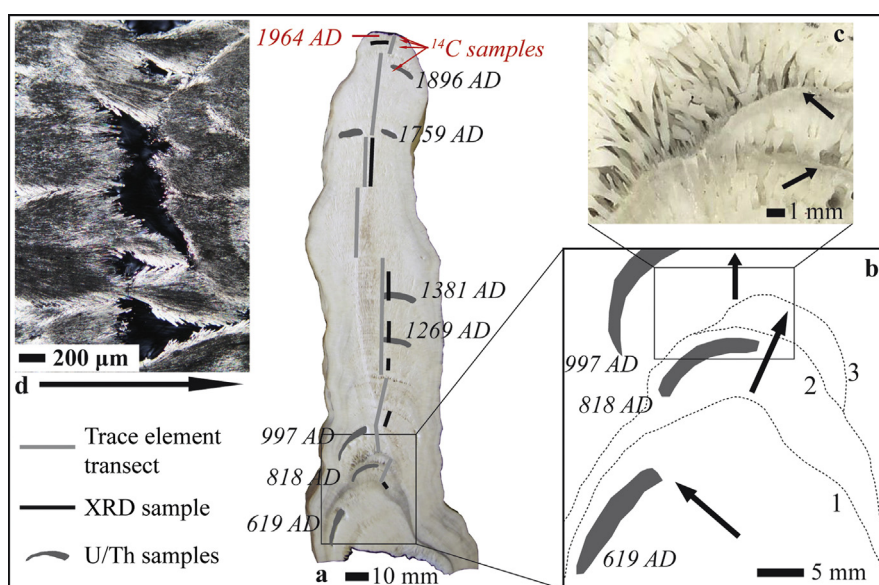


**Fig. 2.** (a) Stalagmite GP5 with U–Th and <sup>14</sup>C derived years, X-ray Diffraction (XRD) sample positions and trace element transects indicated. (b) Sketch showing periods of discontinuous growth labeled 1–3. Changes in drip position caused changes in the growth directions indicated by black arrows. (c) Scan across hiatus surface, note the high porosity directly above the hiatus surface, which provides a 3D-view. Black arrows indicate dense gray layers. (d) Thin section image under crossed nichols showing layering due to alternating low and high porosity layers. Black arrow indicates growth direction.

was used as an internal standard to convert intensities to concentrations (Jochum et al., 2007). Single spots were analyzed every mm (5 yr resolution) for the complete top 20 cm of stalagmite GP5 in order to obtain a high precision. Furthermore, from 1270 to 1330 AD, the stalagmite showed clear layering, which was analyzed at 100  $\mu\text{m}$  resolution (subannual). A relatively large spot size (100  $\mu\text{m}$ ) was used for all measurements to average out heterogeneities within growth increments (Finch et al., 2003; McMillan et al., 2005). The laser had a fluence of 15.7 J/cm<sup>2</sup>. The NIST612 glass and MACS3 carbonate reference materials were used for correction of instrumental biases (Jochum et al., 2012; 2011). The MACS1 reference material (Jochum et al., 2012) was used as a quality control, which demonstrates that relative uncertainties for Mg and Sr are approximately 7%. Sample positions are indicated in Fig. 2. Refer to Jochum et al. (2012, 2007) for details.

Esper et al. (2007) reconstructed PDSI (palmer drought severity index) variations from 1049 to 2001 AD in Morocco. We here include an updated reconstruction by integrating 22 new tree-ring samples collected in 2010 from some of the oldest *Cedrus atlantica* trees in Morocco, “Col du Zad” (Col) in the Middle Atlas. The re-sampling included cedar trees with girth diameters exceeding 4.5 m drilled with a 1 m long increment corer. The new samples were combined with the original collection of 326 tree-ring series detailed in Esper et al. (2007). A sc (self-calibrating) PDSI-reconstruction is derived from linear regression of a combined RCS (regional curve standardization) and linear detrended tree-ring chronology against February–June scPDSI data (van der Schrier et al. 2006) over the period of 1931–2008. Besides increasing replication during earlier periods, the updated scPDSI reconstruction is based on an extended calibration period (now 1931–2008) resulting in an improved transfer model. Using the scPDSI (instead of PDSI; Dai et al., 2004) for calibration has two major advantages: It is (1) based on a finer grid, 0.5° × 0.5° instead of 2.5° × 2.5°, and (2) calibrated with respect to the representative onsite conditions, i.e. reconstructed drought deviations can more directly be compared with variations from other, perhaps

teleconnected regions (van der Schrier et al. 2006). For calibration 40 grid points north of the High Atlas were selected, which represent the synoptic climate setting of the tree-ring sampling sites (see Esper et al. (2007) for detailed information on sampling location and chronology development).

## 4. Results

### 4.1. Updated tree-ring self-calibrating palmer drought Severity index reconstruction

About 50% of the variance retained in the tree-ring based drought reconstruction can be explained by the instrumentally derived scPDSI timeseries ( $r_{1931-2008}=0.69$ ). It shows substantial decadal to centennial scale drought variability from 1043 to 2008 AD, including a pronounced change from dryer conditions during late medieval times to a pluvial period after about 1400 AD (Fig. S3). The past 600 yr were characterized by substantial dry and pluvial swings terminating by a shift towards severe drought in the late 20th century. The scale of PDSI variations also differs between the original and updated reconstructions (Fig. S3), a feature that is largely attributed to the self-calibration process (van der Schrier et al., 2006).

### 4.2. Cave monitoring

At the bottom of the cave, pCO<sub>2</sub> fluctuates between ~450 ppmv (winter) and ~4000 ppmv (summer). In addition, the temperature at the bottom of the cave ranges from 10.7 (winter) to 12.3 °C (summer). Outside air temperature ranges from 7 (winter) to 22 °C (summer). This is strong evidence for seasonally fluctuating cave air ventilation (Bourges et al., 2006; Kowalczyk and Froelich, 2010; Spötl et al., 2005). Speleothem GP5 was collected from the upper cave level (Fig. S2) with a seasonal temperature range between 11.8 °C (winter) and 13.3 °C (summer).

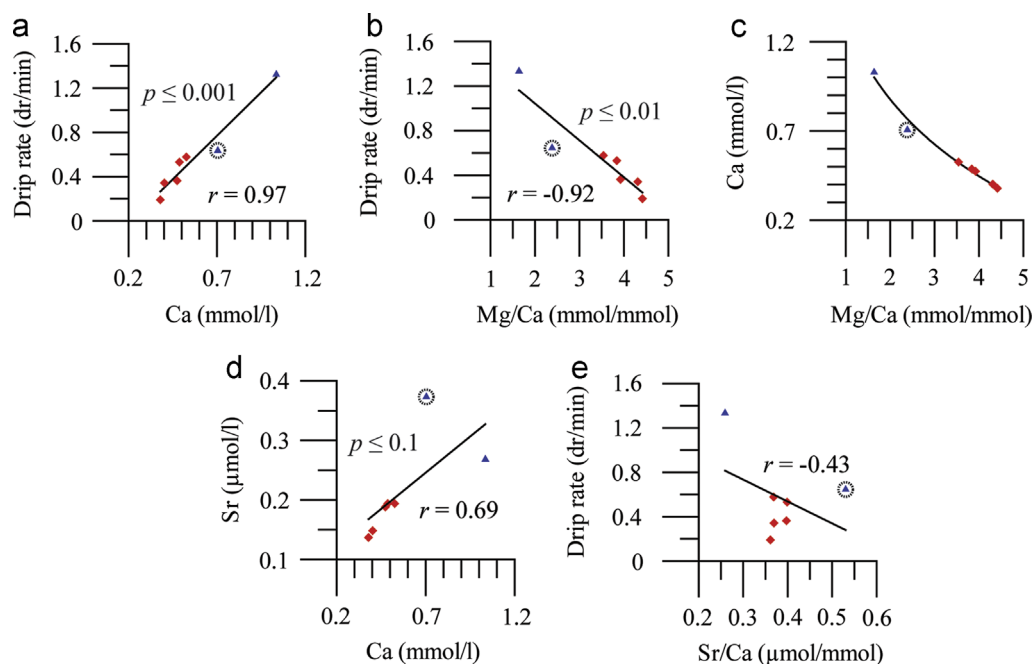


**Fig. 3.** Drip water monitoring data. All elements are expressed in molar concentrations. Blue triangles indicate the samples corresponding to the fastest drip rates. The sample corresponding to the second fastest drip rate is indicated by a dashed circle. Other samples are indicated by a red rhombus. Pearson correlation coefficients and  $p$ -values are indicated. (a) Calcium concentration versus drip rate with linear trend line. (b) Mg/Ca ratio versus drip rate with linear trend line. (c) Mg/Ca ratio versus Ca concentration with exponential trend line, which demonstrates a typical prior CaCO<sub>3</sub> precipitation evolution. (d) Calcium versus Sr concentration with linear trend line. (e) 1000×Sr/Ca versus drip rate with linear trend line. (For interpretation of the references to color in this figure legend, the reader is referred to the web version of this article.)

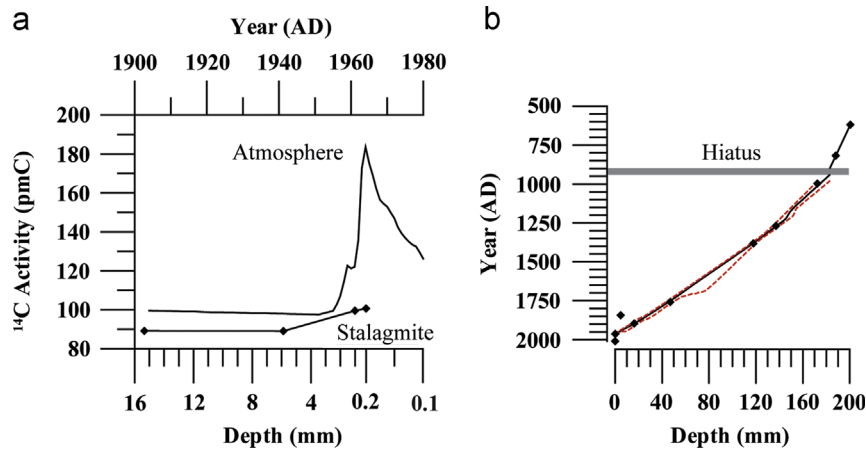


**Fig. 4.** Age-depth model stalagmite GP5. (a) Atmospheric  $^{14}\text{C}$  activity versus stalagmite GP5  $^{14}\text{C}$  activity. The year 1964 AD has been assigned to a depth of 0.2 mm beneath the stalagmite top (2010 AD). (b) Age depth model obtained with StalAge (Scholz and Hoffmann, 2011). Red dashed lines indicate 95%-confidence limits. The age uncertainty of the outlier at 4.8 mm depth was enlarged in order to fit the age depth model according to the estimated position of the  $^{14}\text{C}$  bomb peak. Note that for the basal section linear interpolation was used due to the presence of a hiatus (indicated by the gray bar). Age-uncertainties are not indicated, because they are smaller than the rhombuses (Table S1). (For interpretation of the references to color in this figure legend, the reader is referred to the web version of this article.)

Cave air  $\text{pCO}_2$  has an annually constant mean of  $666 \pm 151$  (1SD) ppmv at the position of stalagmite GP5. Therefore, it is unlikely that variations in cave ventilation had a strong effect on the growth rate of stalagmite GP5.

The drip site which fed stalagmite GP5 has been monitored over a period of 2 yr. Fig. S1 shows that it concerns a drip site with a strong seasonal character with a response to rainfall events as recorded with an automatic drip counter. Highest drip rates (1.3 drip/min) were recorded manually in March 2010 – coinciding with the most negative NAO conditions ever recorded (Osborn, 2011) – and with an automatic drip counter in May 2012 (within a week after a rainfall event). In summer, the drip site is dry (Fig. S1). A strong positive correlation exists between drip rate and drip water Ca concentration. A negative correlation exists between drip rate and drip water Mg/Ca ratio (Fig. 3a and b). This is strong evidence for prior  $\text{CaCO}_3$  precipitation (Fig. 3c; Sinclair et al., 2012). Drip water Mg/Ca ratios are high (generally above two), except for the drip water sample corresponding to the fastest drip rate (Mg/Ca ratio = 1.67). A weak positive correlation between drip water Ca and Sr concentration exists as well (Fig. 3d). The correlation between drip rate and drip water Sr/Ca is not significant (Fig. 3e).

#### 4.3. Age-depth model

The  $^{14}\text{C}$  analysis of four samples indicate significantly elevated  $^{14}\text{C}$  activity in the upper two samples showing that stalagmite GP5 was at least still growing in the early 1960s (Fig. 4a; Table S1). After the 1970s annual rainfall in the Atlantic part of Morocco decreased considerably and induced slow or discontinuous growth. Based on a comparison of the  $^{14}\text{C}$  activity of the stalagmite and an atmospheric  $^{14}\text{C}$  activity curve (Levin and Kromer, 2004; Levin et al., 2010; Reimer et al., 2004), the year 1964 was assigned to a depth of 0.2 mm beneath the stalagmite top (Fig. 4). Although very limited, crystal growth on a watchglass has been observed. This suggests that stalagmite GP5 was actively growing at the time of collection (2010 AD). The year 2010 AD is assigned to the top of stalagmite GP5, and is included in the calculation of the age depth model.

Eight samples were dated by the U–Th method (Table S1). Considering that parts of the  $^{14}\text{C}$  bomb-peak could be identified, one U–Th outlier (close to the stalagmite top; sample GP5 U4; Table S1) was recognized by StalAge (Scholz and Hoffmann, 2011). The error bar for this particular sample was enlarged. The

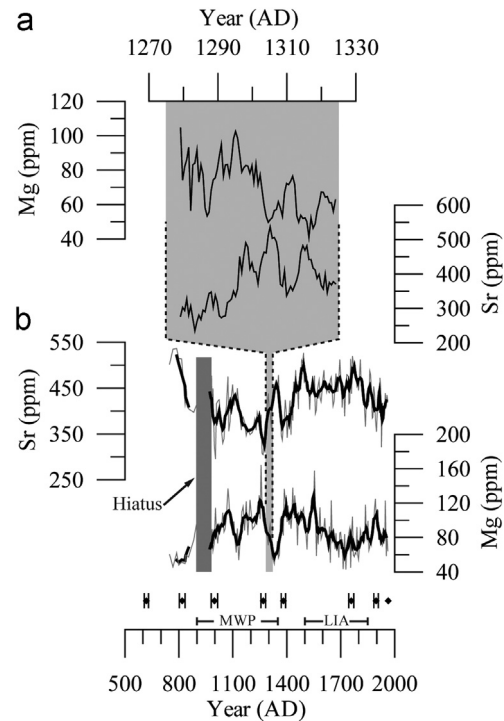


**Fig. 5.** Magnesium and Sr concentrations of stalagmite GP5. (a) 1270–1330 AD, sub-annual resolution. (b) 500–2000 AD, 5 yr resolution. Dark gray bar indicates the position of hiatus. Timing of the Medieval Warm Period (MWP), Little Ice Age (LIA), U–Th ages and the age assigned to 0.2 mm depth due to the  $^{14}\text{C}$  bomb peak are indicated at the bottom of the graph.

stalagmite has a hiatus at 182.7 mm distance from the top (Fig. 2c). For the basal section, constrained by two ages, linear interpolation was used to construct an age model.

The high porosity directly above the hiatus provided a 3-dimensional view of the hiatus surface. From the top it appears as a relatively smooth gray surface (Fig. 2c), whereas in cross section view it appears as a high density gray layer. The higher density is most likely related to a slow down and cease in stalagmite growth. Between 182.7 (hiatus surface) and 195.7 mm from the top, an interval with similar high density gray layers was identified (Fig. 2a–c). These layers coincide with several changes in the drip position inducing changing growth axes and may be

coupled to a period of discontinuous speleothem growth (Fig. 2b). Therefore, the age model of the basal section of the stalagmite is associated with larger uncertainty than the upper section. Discontinuous growth started after 619 ( $\pm 12$  yr) AD, and stalagmite growth ceased at approximately 904 AD. Growth started again between 906 and 982 AD as given by the StalAge algorithm. Between 943 and 1964 AD the stalagmite grew with an average rate of 180  $\mu\text{m}/\text{yr}$ .

#### 4.4. Petrography

Stalagmite GP5 is aragonitic but XRD suggest that minor ( $< 2\%$ ) amounts of calcite are present. The Mg content within the crystal lattice of the subordinate calcite phase ranges from 0.8 to 1.9 mol%. This suggests that calcite co-precipitated with aragonite but was also formed as a secondary phase. Calcite is not recognized in thin sections (Fig. 2d). Aragonite needle crystals show a length to width ratio  $\geq 6:1$  and are organized in fan-like structures, which show a sweeping extinction across several crystals. These are characteristics of an acicular fabric (Frisia and Borsato, 2010). Layering in stalagmite GP5 exists due to more and less porous structures (Fig. 2).

#### 4.5. Geochemistry

Magnesium and Sr concentrations from the 5 yr resolution transect (747–1962 AD) and the sub-annually resolved transect (1270–1330 AD) are presented in Fig. 5. The average concentrations for Mg and Sr are  $87 (\pm 25)$  and  $426 (\pm 49)$  ppm respectively. Between 747 and 1402 AD, Sr is negatively correlated to Mg ( $r_{\text{raw data}} = -0.56$ ,  $r_{5\text{-point running mean}} = -0.78$ ,  $p < 0.001$ ). Between 1402 and 1962 AD, the correlation is weak ( $r_{\text{raw data}} = -0.12$ ,  $r_{5\text{-point running mean}} = -0.24$ ). In addition, the Medieval Warm Period (MWP) is characterized by lower Sr concentrations (394 ppm) compared to the Little Ice Age (LIA; 453 ppm). Strontium decreases towards the hiatus surface, whereas Mg increases (Fig. 5b). The high resolution transect shows opposite patterns for Mg and Sr (Fig. 5a), which are negatively correlated ( $r = -0.54$ ,  $p < 0.001$ ). Porous layers coincide with higher Sr and lower Mg concentrations.

### 5. Climate implications and discussion

Cave monitoring data suggests that the Mg concentration from stalagmite GP5 represents the most sensitive tracer for effective rainfall. Drip water Mg/Ca ratios are most likely reflecting varying amounts of  $\text{CaCO}_3$  precipitation within the karst aquifer or at the cave ceiling in response to changes in climate aridity, i.e. prior calcite precipitation (PCP; Fairchild et al., 2000; Johnson et al., 2006) or prior aragonite precipitation (PAP; Fairchild and Treble, 2009; Wassenburg et al., 2012). However, Mg in aragonitic speleothems can be affected by several processes (Wassenburg et al., 2012), therefore another proxy for effective rainfall has to be included in order to infer robust climate implications.

Strontium concentrations in aragonitic speleothems have formerly been interpreted as a proxy for effective rainfall, where higher (lower) Sr concentrations reflect overall more humid (dry) conditions (Finch et al., 2003; Wassenburg et al., 2012). This relationship seems valid for the GP5 Sr record as well, as indicated by the high coherence with the tree ring scPDSI record on centennial timescales (i.e. the MWP–LIA transition), but also for the high resolution transect (Figs. 6 and 7). Drip water Sr/Ca, however, showed a fairly complex behavior in terms of drip rate. As such, in order to infer robust climate implications both GP5 Sr and Mg concentrations are used.

Note that with respect to GP5's growth rate the spot size used for LA-ICP-MS is relatively small. Therefore, a potential seasonal bias cannot be entirely excluded for single data points, although

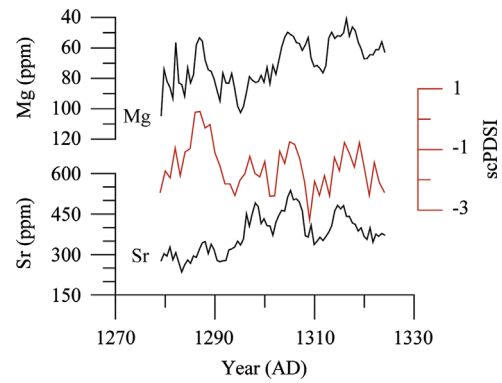


**Fig. 6.** Comparison of non-smoothed high resolution Mg and Sr data from stalagmite GP5 with the self-calibrating (sc) Palmer Drought Severity Index (PDSI) reconstruction (red). (For interpretation of the references to color in this figure legend, the reader is referred to the web version of this article.)

the high resolution Mg and Sr record show very smooth trends in the “raw” data (i.e. no seasonal bias; Fig. 5a). Furthermore, the applied 5 point running mean has a smoothing effect, which averages out the potential seasonal bias. Nevertheless, only the peaks composed of multiple data points from the 5 yr resolution transect are considered to infer climate implications.

#### 5.1. Climate implications

The present debate concerning proxy based reconstructions of the North Atlantic Oscillation (NAO) concerns the non-stationary behavior of the NAO (Jung et al., 2003; Wang et al., 2012) and the stationary character of proxy records (Lehner et al., 2012). Non-stationary behavior of the NAO involves latitudinal or longitudinal shifts of the NAO sea level pressure centers (i.e. the Icelandic Low and the Azores Subtropical High). The  $\text{NAO}_{\text{ms}}$  (Morocco–Scotland) reconstruction from Trouet et al. 2009; (Fig. 7a) is based on two proxy records and may thus be sensitive to NAO non-stationarities. Lehner et al. (2012) re-emphasized several problems with the  $\text{NAO}_{\text{ms}}$  reconstruction, most of which were already mentioned in Trouet et al. (2009): (1) the  $\text{NAO}_{\text{ms}}$  reconstruction from Trouet et al. (2009) fails to verify against NAO-indices from early instrumental measurements from the period before 1900 AD, (2) the shift from positive NAO conditions during the Medieval Warm Period (MWP) to negative NAO conditions during the Little Ice Age (LIA) is not revealed by the climate models and (3) the relatively low variability in the NAO during the MWP was mainly due to the Scottish speleothem record (Fig. 7g). Therefore, the  $\text{NAO}_{\text{ms}}$  reconstruction from Trouet et al. (2009) and the underlying proxy records need further verification.

##### 5.1.1. Multi-centennial climate trends: the MWP–LIA transition

The GP5 Sr record confirms the tree-ring scPDSI reconstruction: the MWP was dominated by overall drier conditions in Morocco, whereas the LIA was wetter (Fig. 7d–f). This is in line with the evidence presented by Détriché et al. (2009) using core data from Lake Afourgagh, located approximately 100 km SW of Grotte de Piste. There, a lake level low stand between 890 and 1201 AD coincides with the MWP. The low stand was bracketed by more humid conditions indicating relatively humid conditions for the LIA in Morocco. On the Iberian Peninsula, a magnetic susceptibility record from the Douro mud patch in NW Portugal (Abrantes et al., 2011) suggests that the MWP was drier compared to the LIA. This has been confirmed by lake and marine proxy records from the Iberian Peninsula (Moreno et al., 2012). Even though some more continental and NW Iberian sites showed more humid conditions during the MWP, the proxy records from Morocco and the Iberian

Peninsula generally agree that the MWP was relatively dry compared to the LIA.

More recently, a long-term NAO reconstruction covering the entire MWP and the transition period to the LIA has been published (Olsen et al., 2012). This reconstruction suggests that the MWP was generally characterized by NAO+ conditions and shows a well pronounced shift towards NAO- conditions at the same time of the scPDSI and GP5 Sr record (Fig. 7; T1). The MWP-LIA transition is also clearly present in a temperature record from the central European Alps (Mangini et al., 2005; Trouet et al., 2009; Fig. 7c). In conclusion, the MWP was generally characterized by NAO+ conditions confirming Trouet et al. (2009). The fact that the transition could not be reproduced by climate models (Lehner et al., 2012) suggests that the climate models need further evaluation.

Another interesting feature in the speleothem record from Scotland is a very clear trend towards more humid conditions from 1760 AD until ~1900 AD (i.e. towards the end of the LIA; Fig. 7g; T2). In terms of NAO dynamics this should coincide with a comparable decrease in rainfall in the Moroccan area. However, Esper et al. (2007) stated that after the LIA, conditions in Morocco continued to be more humid until the 1970s. The GP5 Sr and Mg record show a very clear trend towards drier conditions (Fig. 7d and f; T2). Although potential proxy non-linearities are acknowledged, this may suggest that the NAO<sub>ms</sub> reconstruction from Trouet et al. (2009) is underestimating the amplitude of change within this time interval and could be improved by including other NAO-affected proxy records (Lehner et al., 2012).

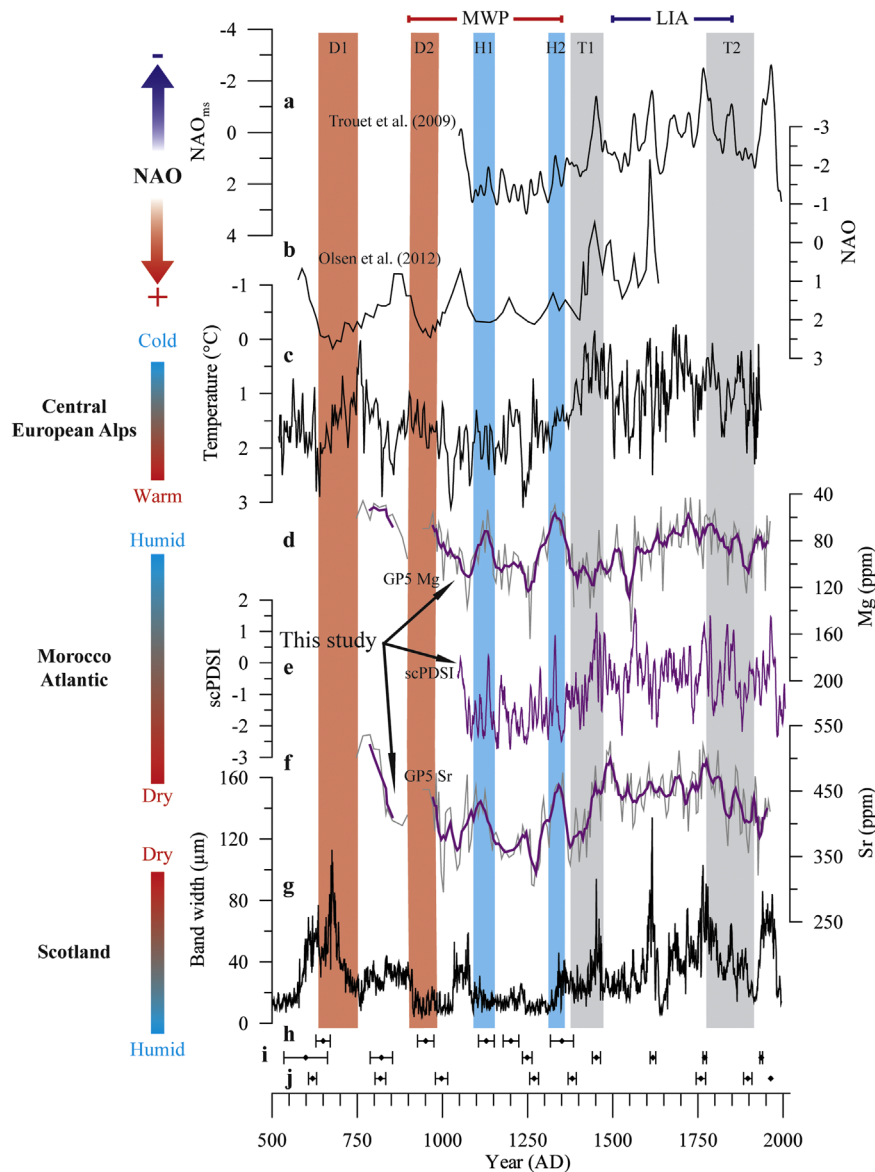


**Fig. 7.** Comparison of Moroccan drought records (stalagmite GP5 Sr and Mg and tree-ring self-calibrating (sc) Palmer Drought Severity Index (PDSI) reconstruction; this study; purple lines; d–f) with: (a) NAO<sub>ms</sub> (North Atlantic Oscillation) reconstruction from Trouet et al. (2009), (b) NAO reconstruction from West Greenland (Olsen et al., 2012), (c) temperature reconstruction from Spannagel Cave (Central European Alps; Mangini et al., 2005), (g) speleothem band width record from Scotland (Proctor et al., 2002), (h–j) dating positions and uncertainties corresponding to the NAO reconstruction from Olsen et al. (2012), the temperature reconstruction from Mangini et al. (2005) and stalagmite GP5 from Morocco, respectively. Dry periods in Morocco as recognized in stalagmite GP5 are indicated by the red bars labeled D1 and D2. Wet periods during the Medieval Warm Period (MWP) as recognized in stalagmite GP5 Mg and Sr records are indicated by the blue bars labeled H1 and H2. Transition zones in stalagmite GP5 are indicated by the gray bars labeled T1 and T2. Timing of the Medieval Warm Period (MWP) and the Little Ice Age (LIA) is indicated. (For interpretation of the references to color in this figure legend, the reader is referred to the web version of this article.)

### 5.1.2. (Multi-) decadal climate variability: 619–1400 AD

Although the MWP was generally characterized by NAO+ conditions, the persistence of NAO+ conditions (i.e. its low variability), as suggested by the Trouet  $NAO_{ms}$ , remains a point of discussion. As correctly mentioned by Lehner et al. (2012) this low variability is mainly related to the Scottish speleothem record (Fig. 7g). Proctor et al. (2002) also mentioned that the Scottish speleothem record may respond non-linear to changes in rainfall during already humid conditions, explaining the apparent low NAO variability during the MWP. Even though the NAO reconstruction from West Greenland (Olsen et al., 2012) seems to confirm the Trouet  $NAO_{ms}$  reconstruction in this aspect (Fig. 7a and b), the GP5 Mg and Sr records indicate at least two wet phases in Morocco (Fig. 7d and f; H1 and H2). These overlap with two peaks in the scPDSI reconstruction (Fig. 7d–f), although the wet phases in GP5 appear to cover a longer time period. The first wet period (indicated as H1 in Fig. 7) centered around 1120 AD

coincides with wet periods recorded in the Douro mud patch (Abrantes et al., 2011), and lake records from the Iberian Peninsula (lake Arreos, Estanya, Basa de la Mora; Moreno et al., 2012), suggesting a regional response to large scale atmospheric circulation patterns most likely related to NAO- conditions. However, this is not supported by either the West Greenland NAO reconstruction or the Scottish speleothem. The second wet phase, which marks the end of the MWP (H2 in Fig. 7) has not been recorded in the Iberian Peninsula but does coincide with NAO- conditions in the West Greenland NAO record. These inconsistencies might be explained by non-stationary behavior of the NAO (Jung et al., 2003; Lehner et al., 2012; Wang et al., 2012). It can thus be suggested that the  $NAO_{ms}$  reconstruction from Trouet et al. (2009) has underestimated the variability during the MWP.

Stalagmite GP5 shows a period of discontinuous growth shortly after 619 AD ending after a hiatus around 940 AD (Fig. 7; D1–D2). The beginning of discontinuous growth (Fig. 7; D1) most likely

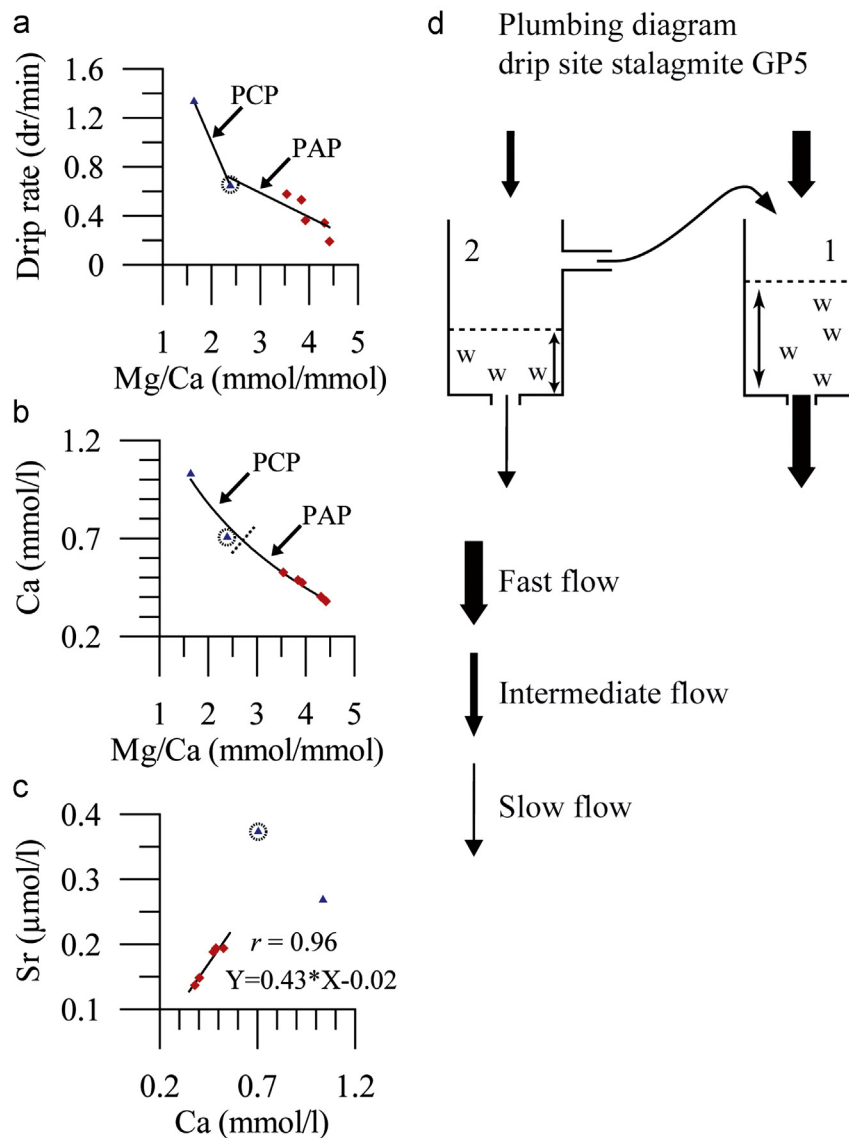


**Fig. 8.** Drip water monitoring data with indication of dominance of prior calcite precipitation (PCP) and prior aragonite precipitation (PAP). Blue triangles indicate drip water samples corresponding to the two fastest drip rates. The blue triangle with a dashed circle corresponds to the second fastest drip rate, other samples are indicated by a red rhombus. All elements are expressed in molar concentrations. Pearson correlation coefficients and  $p$ -values are indicated. (a) Drip rate versus Mg/Ca ratio. (b) Ca versus Mg/Ca ratio. (c) Drip water Sr versus Ca concentration, with trend line based on the five samples corresponding to the slowest drip rates and highest drip water Mg/Ca ratios. Equation of the trend line is given. (d) Simplified plumbing diagram of stalagmite GP5's drip site (modified after Fairchild et al., 2006). Reservoir no. 1 is the main contributor to the discharge at GP5's drip site. (For interpretation of the references to color in this figure legend, the reader is referred to the web version of this article.)

indicates increasingly arid conditions in Morocco, potentially related to NAO+ conditions. Indeed, the beginning of discontinuous growth in stalagmite GP5 seems to coincide with the strongest NAO+ conditions of the last 5.200 yr (Olsen et al., 2012). Furthermore, the moderately-well dated hiatus (Fig. 7d and f; D2) at the very least overlaps with the NAO+ conditions around 950 AD as found in West Greenland (Olsen et al., 2012). Overall, the West Greenland NAO reconstruction confirms that the dry periods in Morocco indicated by stalagmite GP5 (D1 and D2 in Fig. 7) result from NAO+ conditions.

The lack of a clear multi-decadal coherence between the temperature reconstruction of the central European Alps during the MWP (Mangini et al., 2005) and the GP5 record or the West Greenland NAO reconstruction (Olsen et al., 2012) suggests that the temperature in the central European Alps is not always sensitive to changes in the state of the NAO (Fig. 7c). It also appears that the Scottish speleothem record indicates drier conditions during the strongest NAO+ conditions of the last 5.200 yr (Fig. 7g). This might be explained by its sensitivity to temperature changes in addition to changes in rainfall (Proctor et al., 2002, 2000). Moreover, extreme NAO+ conditions are able to induce both higher temperatures and very wet conditions in the area of NW Scotland. The sensitivity to changes in rainfall decreases under very wet conditions (Proctor et al., 2002). During these periods, temperature changes may be more dominant.

## 5.2. Processes controlling Mg and Sr in speleothem GP5

### 5.2.1. Prior calcite precipitation versus prior aragonite precipitation

In calcitic speleothems positive correlations of Mg and Sr have often been related to varying amounts of PCP, whereas higher Mg and Sr concentrations were related to lower effective rainfall (Johnson et al., 2006). The potential effects of PCP and PAP on stalagmite Mg and Sr concentrations are considerably different due to the different distribution coefficients. In an unlimited reservoir:

$$(D_{\text{trace}} = (\text{trace}/\text{Ca})_{\text{solid}}/(\text{trace}/\text{Ca})_{\text{solution}}), \quad (1)$$

where  $(\text{trace}/\text{Ca})_{\text{solid}}$  and  $(\text{trace}/\text{Ca})_{\text{solution}}$  are the trace element to Ca ratio in the precipitated mineral and the solution, respectively. For calcite  $D_{\text{Mg}}=0.019$  and  $D_{\text{Sr}}=0.072$  at 15 °C (Huang and Fairchild, 2001), where  $D_{\text{Mg}}$  has a dependence on temperature (Huang and Fairchild, 2001; Oomori et al., 1987).  $D_{\text{Sr}}$  is also controlled by crystal growth rate (Lorens, 1981; Tang et al., 2008; Treble et al., 2005). For aragonite,  $D_{\text{Mg}}$  is one or more orders of magnitude smaller with a dependence on crystal growth rate (i.e.  $0.00002 \leq D_{\text{Mg}} \leq 0.00008$ ; Gabitov et al., 2008) although higher  $D_{\text{Mg}}$  values have been published as well (i.e.  $D_{\text{Mg}} \approx 0.0007$  or  $0.0017$ ; Gaetani and Cohen, 2006; Zhong and Mucci, 1989).  $D_{\text{Sr}}$  is several orders of magnitude larger (i.e.  $D_{\text{Sr}} \approx 1.2$ ; Dietzel et al., 2004; Gaetani and Cohen, 2006). According to Zhong and Mucci (1989)  $D_{\text{Sr}}$  does not depend on growth rate significantly. Note that only Huang and Fairchild (2001) performed precipitation experiments under cave analog conditions, for aragonite such experiments are not available.

Because  $D_{\text{Mg}}$  and  $D_{\text{Sr}}$  are both far below one for calcite precipitation, enhanced PCP during increasingly arid conditions will increase the drip water Mg/Ca and Sr/Ca ratios and thus induce a positive correlation between stalagmite Mg and Sr concentrations. In the case of PAP, however,  $D_{\text{Mg}}$  is far below one whilst  $D_{\text{Sr}}$  is slightly above one. Enhanced PAP may thus increase the drip water Mg/Ca ratio, but decrease the drip water Sr/Ca ratio. Prior aragonite precipitation may thus be able to induce negative correlations between stalagmite Mg and Sr concentrations.

Precipitation of aragonite in cave environments has often been related to high drip water Mg/Ca ratios (Frisia et al., 2002;

McMillan et al., 2005; Wassenburg et al., 2012). Estimations of molar drip water Mg/Ca ratios required to precipitate aragonite vary from 1.2 to 3.3 (Frisia et al., 2002; Niedermayr et al., 2013; Railsback et al., 1994; Wassenburg et al., 2012). Under increasingly dry conditions, it appears likely that PCP increases the drip water Mg/Ca ratio to such an extent that PAP takes over. This scenario may be especially valid for Grotte de Piste as the dolostone host rock provides a high background drip water Mg/Ca ratio, therefore only little amounts of PCP are necessary to induce the precipitation of aragonite (Wassenburg et al., 2012). As explained above, the potential switch from PCP to PAP may have significant impacts on the interpretation of particularly the Sr record. It has to be noted, however, that  $\text{CO}_2$  degassing rates, temperature,  $\text{CaCO}_3$  saturation state and  $\text{CO}_3^{2-}$  controlled kinetic effects affect the drip water Mg/Ca threshold (De Choudens-Sanchez and Gonzalez, 2009; Fernández-Díaz et al., 1996; Niedermayr et al., 2013; Zuddas and Mucci, 1998).

### 5.2.2. Evidence for prior aragonite precipitation

Strontium represents the most sensitive element for distinguishing PAP from PCP. This is due to the fact that  $D_{\text{Sr}}$  is higher than one for aragonite precipitation, but far below one for calcite precipitation. In the case of PAP, a positive correlation between drip water Sr and Ca concentrations can be expected. Prior calcite precipitation may induce a nearly horizontal trend line, because only little Sr is incorporated by calcite. In Fig. 3d it appeared that only a weak positive correlation existed between drip water Sr and Ca concentration. This is mainly related to the two drip water samples, which correspond to the highest drip rates and highest Sr concentrations (Fig. 8c). By plotting drip water Sr versus Ca concentrations, it is possible to calculate a  $D_{\text{Sr}}$  corresponding to the  $\text{CaCO}_3$  polymorph that caused the depletion in drip water Sr and Ca (assuming that initial drip water Sr/Ca ratios are constant). The slope indicates how much Sr is taken out from the solution with respect to Ca, i.e. how much has been incorporated into the respective  $\text{CaCO}_3$  polymorph. The  $D_{\text{Sr}}$  can then be derived by dividing the slope of the trend line by a measured drip water Sr/Ca value. When the two Sr values corresponding to the two fastest drip rates are excluded for the calculation of the trend line, Sr and Ca show a strong significant positive correlation (Fig. 8c). The calculated  $D_{\text{Sr}}$  ranges from 1.08 to 1.2 (depending on the drip water sample), which is very close to values from inorganic aragonite precipitation experiments ( $\sim 1.2$ ; Dietzel et al., 2004; Gaetani and Cohen, 2006). This suggests that GP5's drip site is indeed associated with PAP.

The first reason to exclude the samples with the two highest drip water Sr concentrations is the fact that they are characterized by the lowest drip water Mg/Ca ratios (i.e. 1.67 and 2.39), these Mg/Ca ratios are not necessarily sufficient to induce PAP, drip water may thus still be dominated by PCP (Fig. 8a and b). In addition, the two samples with the highest drip water Sr concentrations represent the effect of an anomalously wet winter season related to the most extreme NAO- conditions ever recorded (Osborn, 2011). It is possible, that a second karst water reservoir enriched in Sr contributes to the main drip water (Baker et al., 2000; Fairchild et al., 2006) after multiple days with strong precipitation events (i.e. the second reservoir is characterized by a recharge threshold). This is an often described phenomenon in cave monitoring studies and is referred to as "piston flow" (Fuller et al., 2008; Karmann et al., 2007; Tooth and Fairchild, 2003). The fact that the second fastest drip has the highest drip water Sr concentration may suggest that the recharge of the second reservoir is delayed with respect to the main reservoir (Fig. 8d). This assumption requires confirmation by a highly time-resolved monitoring program.

A negative correlation between stalagmite Mg and Sr was identified for the dry MWP. This may indicate that variable amounts of PAP have been recorded. Periods of strong rainfall events probably induced a larger piston flow component, which forced the drip water Sr/Ca ratio in the same direction as a reduction of PAP. The small delay in piston flow after periods with several extreme precipitation events may cause lower drip water Sr/Ca ratios. However, it is argued that in general the high Sr concentrations in stalagmite GP5 during the LIA are related to a combination of reduced PAP and an increase in the amount of Sr-enriched water through piston flow. It may even be the case that the LIA is dominated by PCP or alternations of PCP and PAP, complicating the interpretation of multi-decadal climate variability for this wet period.

### 5.2.3. Magnesium in aragonite speleothems

$D_{\text{Mg}}$  for aragonite is small, such that aragonite incorporates only trace amounts of Mg. Most of the Mg may be incorporated through absorption of the ions or clay minerals on the crystal surface, which may get “trapped” in the case that crystal growth is fast enough (Watson, 2004). Gabitov et al. (2008) also suggested that this mechanism caused the observed growth rate effects. Clay minerals absorb Mg due to charge deficits in their crystal structure (Brigatti et al., 2006). In a dolomitic karst aquifer, Mg and Ca ions are dominating the drip water. Therefore clay minerals in this system will be “packed” with Mg and Ca ions. Clay minerals may thus disturb the climate signal from PCP or PAP in speleothem Mg concentrations. More specifically, the incorporation of clay minerals may mimic a dry climate signal in the speleothem record. Another potential effect on Mg concentrations in aragonite speleothems is related to primary co-precipitating calcite. Two percent of primary calcite may already induce a 200 ppm increase in Mg (Wassenburg et al., 2012).

With reference to stalagmite GP5, XRD data suggest that the effects of primary co-precipitating calcite are negligible. Growth rate effects on the GP5 Mg record may be visible on seasonal, but not on decadal timescales. This is because the growth rate in stalagmite GP5 is nearly constant over the last 1000 yr with a mean of 180  $\mu\text{m}/\text{yr}$  until the 1970s (Fig. 4b). Clay minerals may be indicated by peak concentrations of Al, which is a major constituent of clay. GP5 Al concentrations appear to affect the Mg record from approximately the beginning of the LIA (Fig. S4). This explains the lack of a clear MWP–LIA transition in the Mg record of GP5. Overall, the GP5 Mg record during the MWP was mainly controlled by PCP and PAP.

## 6. Conclusions

The Medieval Warm Period (MWP) was generally characterized by positive North Atlantic Oscillation (NAO) conditions in comparison to the little ice age (LIA). This has been demonstrated by a new stalagmite record and an updated scPDSI reconstruction from Morocco combined with multiple records from the Iberian Peninsula and a NAO reconstruction from West Greenland, confirming the NAO reconstruction from Trouet et al. (2009). During the MWP, a considerable variability in rainfall has been documented in Morocco and the Iberian Peninsula. These findings supplement the Trouet et al. (2009)  $\text{NAO}_{\text{ms}}$  reconstruction suggesting overall more variable NAO conditions during the MWP. In stalagmite GP5, discontinuous growth – interpreted as the initiation of a dry phase in Morocco – started after 619 AD and coincided with the most extreme  $\text{NAO}^+$  conditions as observed in the West Greenland NAO reconstruction. Also, a second dry phase in Morocco around 940 AD, reflected in a hiatus in stalagmite GP5, has been related to  $\text{NAO}^+$  conditions.

Monitoring data of drip water Mg/Ca and Sr/Ca ratios from a drip site with an actively growing aragonite stalagmite document that prior aragonite precipitation (PAP) has a substantially different impact on speleothem aragonite Sr concentrations relative to prior calcite precipitation (PCP). Prior aragonite precipitation, driven by increased aridity, is able to induce negative correlations between Mg and Sr in aragonitic speleothems. Higher Sr and lower Mg concentrations indicate lower amounts of PAP. Magnesium concentrations in aragonite speleothems may be compromised by Mg-bearing clay minerals incorporated through absorption on the crystal surface.

## Acknowledgments

This work was financed by the Deutsche Forschungsgemeinschaft (DFG; Project IM 44/1). We would like to thank the following people for fruitful discussions and support: A. Borsato, C. Spötl, D. Fleitmann, U. Weis, B. Stoll, D. Buhl, B. Gehnen, T. Reinecke, H.-J. Bernard, I. Sadalmelik, Mileud, H. Mansouri, T. Echchibi, M. Born and A. Schulz. Finally, we would like to thank H. Stoll and two anonymous reviewers for their constructive comments, which improved the manuscript significantly. The editorial handling of the manuscript by G. Henderson is gratefully acknowledged.

## Appendix A. Supplementary information

Supplementary data associated with this article can be found in the online version at <http://dx.doi.org/10.1016/j.epsl.2013.05.048>.

## References

- Abrantes, F., Rodrigues, T., Montanari, B., Santos, C., Witt, L., Lopes, C., Voelker, A.H.L., 2011. Climate of the last millennium at the southern pole of the North Atlantic Oscillation: an inner-shelf sediment record of flooding and upwelling. *Clim. Res.* 48, 261–280.
- Baker, A., Genty, D., Fairchild, I.J., 2000. Hydrological characterisation of stalagmite dripwaters at Grotte de Villars, Dordogne, by the analysis of inorganic species and luminescent organic matter. *Hydrol. Earth Syst. Sci.* 4, 439–449.
- Bertaux, J., Sondag, F., Santos, R., Soubiès, F., Causse, C., Plagnes, V., Le Cornec, F., Seidel, A., 2002. Paleoclimatic record of speleothems in a tropical region: study of laminated sequences from a Holocene stalagmite in Central-West Brazil. *Quat. Int.* 89, 3–16.
- Bourges, F., Genthon, P., Mangin, A., D’Hulst, D., 2006. Microclimates of L’Aven d’Orgnac and other French limestone caves (Chauvet, Esparros, Marsoulas). *Int. J. Climatol.* 26, 1651–1670.
- Brigatti, M.F., Galan, E., Theng, B.K.G., 2006. Structures and mineralogy of clay minerals. In: Bergaya, F., Theng, B.K.G., Lagaly, G. (Eds.), *Handbook of Clay Science, Developments in Clay Science*. Elsevier, Amsterdam, pp. 19–86.
- Cai, Y.J., Tan, L.C., Cheng, H., An, Z.S., Edwards, R.L., Kelly, M.J., Kong, X.G., Wang, X.F., 2010. The variation of summer monsoon precipitation in central China since the last deglaciation. *Earth Planet. Sci. Lett.* 291, 21–31.
- Cook, E.R., D’Arrigo, R.D., Mann, M.E., 2002. A well-verified, multiproxy reconstruction of the winter North Atlantic Oscillation index since AD 1400. *J. Clim.* 15, 1754–1764.
- Cosford, J., Qing, H.R., Eglinton, B., Matthey, D., Yuan, D.X., Zhang, M.L., Cheng, H., 2008. East Asian monsoon variability since the Mid-Holocene recorded in a high-resolution, absolute-dated aragonite speleothem from eastern China. *Earth Planet. Sci. Lett.* 275, 296–307.
- Cruz, F.W., Burns, S.J., Karmann, I., Sharp, W.D., Vuille, M., Cardoso, A.O., Ferrari, J.A., Dias, P.L.S., Viana, O., 2005. Insolation-driven changes in atmospheric circulation over the past 116,000 years in subtropical Brazil. *Nature* 434, 63–66.
- Dai, A., Trenberth, K.E., Qian, T.T., 2004. A global dataset of Palmer Drought Severity Index for 1870–2002: relationship with soil moisture and effects of surface warming. *J. Hydrometeorol.* 5, 1117–1130.
- De Choudens-Sanchez, V., Gonzalez, L.A., 2009. Calcite and aragonite precipitation under controlled instantaneous supersaturation: elucidating the role of  $\text{CaCO}_3$  saturation state and Mg/Ca ratio on calcium carbonate polymorphism. *J. Sediment. Res.* 79, 363–376.
- Détriché, S., Bréheret, J.G., Soulié-Marsche, I., Kerrat, L., Maccare, J.J., 2009. Late Holocene water level fluctuations of Lake Afouargagh (Middle-Atlas Mountains,

- Morocco) inferred from charophyte remains. *Paleogeogr. Paleoclimatol. Paleocool.* 283, 134–147.
- Dietzel, M., Gussone, N., Eisenhauer, A., 2004. Co-precipitation of Sr<sup>2+</sup> and Ba<sup>2+</sup> with aragonite by membrane diffusion of CO<sub>2</sub> between 10 and 50 °C. *Chem. Geol.* 203, 139–151.
- Drysdale, R.N., Hellstrom, J.C., Zanchetta, G., Fallick, A.E., Goni, M.F.S., Couchoud, I., McDonald, J., Maas, R., Lohmann, G., Isola, I., 2009. Evidence for obliquity forcing of glacial termination II. *Science* 325, 1527–1531.
- Esper, J., Frank, D., Buntgen, U., Verstege, A., Luterbacher, J., 2007. Long-term drought severity variations in Morocco. *Geophys. Res. Lett.* 34, 5.
- Fairchild, I.J., Borsato, A., Tooth, A.F., Frisia, S., Hawkesworth, C.J., Huang, Y.M., McDermott, F., Spiro, B., 2000. Controls on trace element (Sr–Mg) compositions of carbonate cave waters: implications for speleothem climatic records. *Chem. Geol.* 166, 255–269.
- Fairchild, I.J., Treble, P.C., 2009. Trace elements in speleothems as recorders of environmental change. *Quat. Sci. Rev.* 28, 449–468.
- Fairchild, I.J., Tuckwell, G.W., Baker, A., Tooth, A.F., 2006. Modelling of dripwater hydrology and hydrogeochemistry in a weakly karstified aquifer (Bath, UK): implications for climate change studies. *J. Hydrol.* 321, 213–231.
- Fernández-Díaz, L., Putnis, A., Prieto, M., Putnis, C.V., 1996. The role of magnesium in the crystallization of calcite and aragonite in a porous medium. *J. Sediment. Res.* 66, 482–491.
- Fietzke, J., Liebetrau, V., Eisenhauer, A., Dullo, C., 2005. Determination of uranium isotope ratios by multi-static MIC-ICP-MS: method and implementation for precise U- and Th-series isotope measurements. *J. Anal. At. Spectrom.* 20, 395–401.
- Finch, A.A., Shaw, P.A., Holmgren, K., Lee-Thorp, J., 2003. Corroborated rainfall records from aragonitic stalagmites. *Earth Planet. Sci. Lett.* 215, 265–273.
- Finch, A.A., Shaw, P.A., Weedon, G.P., Holmgren, K., 2001. Trace element variation in speleothem aragonite: potential for palaeoenvironmental reconstruction. *Earth Planet. Sci. Lett.* 186, 255–267.
- Fohlmeister, J., Schroder-Ritzrau, A., Scholz, D., Riechelmann, D.F.C., Mudelsee, M., Wackerbarth, A., Gerdes, A., Riechelmann, S., Immenhauser, A., Richter, D.K., Mangini, A., 2012. Bunker Cave stalagmites: an archive for central European Holocene climate variability. *Clim. Past* 8, 1751–1764.
- Frisia, S., Borsato, A., 2010. Karst. In: Alonso-Zarza, A.M., Tanner, L.H. (Eds.), *Carbonates in Continental Settings—Facies, Environments and Processes, Developments in Sedimentology*, vol. 61. Elsevier, pp. 269–318.
- Frisia, S., Borsato, A., Fairchild, I.J., McDermott, F., Selmo, E.M., 2002. Aragonite–calcite relationships in speleothems (Grotte de Clamouse, France): environment, fabrics, and carbonate geochemistry. *J. Sediment. Res.* 72, 687–699.
- Frisia, S., Fairchild, I.J., Fohlmeister, J., Miorandi, R., Spötl, C., Borsato, A., 2011. Carbon mass-balance modelling and carbon isotope exchange processes in dynamic caves. *Geochim. Cosmochim. Acta* 75, 380–400.
- Füchtbauer, H., Richter, D.K., 1988. Karbonatgesteine. In: Füchtbauer, H. (Ed.), *Sedimente und Sedimentgesteine*. Schweizerbart'sche Verlagsbuchhandlung, Stuttgart, pp. 233–434.
- Fuller, L., Baker, A., Fairchild, I.J., Spötl, C., Marca-Bell, A., Rowe, P., Dennis, P.F., 2008. Isotope hydrology of dripwaters in a Scottish cave and implications for stalagmite palaeoclimate research. *Hydrol. Earth Syst. Sci.* 12, 1065–1074.
- Gabitov, R.I., Gaetani, G.A., Watson, E.B., Cohen, A.L., Ehrlich, H.L., 2008. Experimental determination of growth rate effect on U<sup>6+</sup> and Mg<sup>2+</sup> partitioning between aragonite and fluid at elevated U<sup>6+</sup> concentration. *Geochim. Cosmochim. Acta* 72, 4058–4068.
- Gaetani, G.A., Cohen, A.L., 2006. Element partitioning during precipitation of aragonite from seawater: a framework for understanding paleoproxies. *Geochim. Cosmochim. Acta* 70, 4617–4634.
- Genty, D., Massault, M., 1999. Carbon transfer dynamics from bomb-C-14 and delta C-13 time series of a laminated stalagmite from SW France—modelling and comparison with other stalagmite records. *Geochim. Cosmochim. Acta* 63, 1537–1548.
- Hodge, E., McDonald, J., Fischer, M., Redwood, D., Hua, Q., Levchenko, V., Drysdale, R., Waring, C., Fink, D., 2011. Using the (14)C bomb pulse to date young speleothems. *Radiocarbon* 53, 345–357.
- Holmgren, K., Karlen, W., Lauritzen, S.E., Lee-Thorp, J.A., Partridge, T.C., Piketh, S., Repinski, P., Stevenson, C., Svanered, O., Tyson, P.D., 1999. A 3000-year high-resolution stalagmite-based record of palaeoclimate for northeastern South Africa. *Holocene* 9, 295–309.
- Holzkämper, S., Holmgren, K., Lee-Thorp, J., Talma, S., Mangini, A., Partridge, T., 2009. Late Pleistocene stalagmite growth in Wolkberg Cave, South Africa. *Earth Planet. Sci. Lett.* 282, 212–221.
- Huang, Y.M., Fairchild, I.J., 2001. Partitioning of Sr<sup>2+</sup> and Mg<sup>2+</sup> into calcite under karst-analogue experimental conditions. *Geochim. Cosmochim. Acta* 65, 47–62.
- Hurrell, J.W., 1995. Decadal trends in the North-Atlantic Oscillation—regional temperatures and precipitation. *Science* 269, 676–679.
- Hurrell, J.W., 1996. Influence of variations in extratropical wintertime teleconnections on Northern Hemisphere temperature. *Geophys. Res. Lett.* 23, 665–668.
- Hurrell, J.W., Van Loon, H., 1997. Decadal variations in climate associated with the north Atlantic oscillation. *Clim. Change* 36, 301–326.
- Jochum, K.P., Scholz, D., Stoll, B., Weis, U., Wilson, S.A., Yang, Q., Schwalb, A., Börner, N., Jacob, D.E., Andreae, M.O., 2012. Accurate trace element analysis of speleothems and biogenic calcium carbonates by LA-ICP-MS. *Chem. Geol.* 318, 31–44.
- Jochum, K.P., Stoll, B., Herwig, K., Willbold, M., 2007. Validation of LA-ICP-MS trace element analysis of geological glasses using a new solid-state 193 nm Nd: YAG laser and matrix-matched calibration. *J. Anal. At. Spectrom.* 22, 112–121.
- Jochum, K.P., Weis, U., Stoll, B., Kuzmin, D., Yang, Q., Raczek, I., Jacob, D.E., Stracke, A., Birbaum, K., Frick, D.A., Günther, D., Enzweiler, J., 2011. Determination of reference values for NIST SRM 610–617 glasses following ISO guidelines. *Geostand. Geoanal. Res.* 35, 397–429.
- Johnson, K.R., Hu, C.Y., Belshaw, N.S., Henderson, G.M., 2006. Seasonal trace-element and stable-isotope variations in a Chinese speleothem: the potential for high-resolution paleomonsoon reconstruction. *Earth Planet. Sci. Lett.* 244, 394–407.
- Jung, T., Hilmer, M., Ruprecht, E., Kleppek, S., Gulev, S.K., Zolina, O., 2003. Characteristics of the recent eastward shift of interannual NAO variability. *J. Clim.* 16, 3371–3382.
- Kanner, L.C., Burns, S.J., Cheng, H., Edwards, R.L., 2012. High-latitude forcing of the South American summer monsoon during the last glacial. *Science* 335, 570–573.
- Karmann, I., Cruz, F.W., Viana, O., Burns, S.J., 2007. Climate influence on geochemistry parameters of waters from Santana-Perolas cave system, Brazil. *Chem. Geol.* 244, 232–247.
- Knippertz, P., Christoph, M., Speth, P., 2003. Long-term precipitation variability in Morocco and the link to the large-scale circulation in recent and future climates. *Meteorology and Atmospheric Physics* 83, 67–88.
- Kowalczyk, A.J., Froelich, P.N., 2010. Cave air ventilation and CO<sub>2</sub> outgassing by radon-222 modeling: how fast do caves breathe? *Earth Planet. Sci. Lett.* 289, 209–219.
- Lehner, F., Raible, C.C., Stocker, T.F., 2012. Testing the robustness of a precipitation proxy-based North Atlantic Oscillation reconstruction. *Quat. Sci. Rev.* 45, 85–94.
- Levin, I., Kromer, B., 2004. The tropospheric <sup>14</sup>CO<sub>2</sub> level in mid-latitudes of the Northern Hemisphere (1959–2003). *Radiocarbon* 46, 1261–1272.
- Levin, I., Naegler, T., Kromer, B., Diehl, M., Francey, R.J., Gomez-Pelaez, A.J., Steele, L. P., Wagenbach, D., Weller, R., Worthly, D.E., 2010. Observations and modelling of the global distribution and long-term trend of atmospheric <sup>14</sup>CO<sub>2</sub>. *Tellus Ser. B Chem. Phys. Meteorol.* 62, 26–46.
- Li, T.Y., Shen, C.C., Li, H.C., Li, J.Y., Chiang, H.W., Song, S.R., Yuan, D.X., Lin, C.D.J., Gao, P., Zhou, L.P., Wang, J.L., Ye, M.Y., Tang, L.L., Xie, S.Y., 2011. Oxygen and carbon isotopic systematics of aragonite speleothems and water in Furong Cave, Chongqing, China. *Geochim. Cosmochim. Acta* 75, 4140–4156.
- Lorenz, R.B., 1981. Sr, Cd, Mn and Co distribution coefficients in calcite as a function of calcite precipitation rate. *Geochim. Cosmochim. Acta* 45, 553–561.
- Luterbacher, J., Schmutz, C., Gyalistras, D., Xoplaki, E., Wanner, H., 1999. Reconstruction of monthly NAO and EU indices back to AD 1675. *Geophys. Res. Lett.* 26, 2745–2748.
- Mangini, A., Spötl, C., Verdes, P., 2005. Reconstruction of temperature in the Central Alps during the past 2000 yr from a delta O-18 stalagmite record. *Earth Planet. Sci. Lett.* 235, 741–751.
- Martin-García, R., Alonso-Zarza, A.M., Martín-Pérez, A., 2009. Loss of primary texture and geochemical signatures in speleothems due to diagenesis: evidences from Castanar cave, Spain. *Sediment. Geol.* 221, 141–149.
- Mattey, D., Lowry, D., Duffet, J., Fisher, R., Hodge, E., Frisia, S., 2008. A 53 year seasonally resolved oxygen and carbon isotope record from a modern Gibraltar speleothem: reconstructed drip water and relationship to local precipitation. *Earth Planet. Sci. Lett.* 269, 80–95.
- McMillan, E.A., Fairchild, I.J., Frisia, S., Borsato, A., McDermott, F., 2005. Annual trace element cycles in calcite–aragonite speleothems: evidence of drought in the western Mediterranean 1200–1100 yr BP. *J. Quat. Sci.* 20, 423–433.
- Miao, S.J., d'Aloncourt, R.N., Reinecke, T., Kasatkina, I., Behrens, M., Schögl, R., Muhler, M., 2009. A study of the influence of composition on the microstructural properties of ZnO/Al(2)O(3) mixed oxides. *Eur. J. Inorg. Chem.* 910–921 <http://dx.doi.org/10.1002/ejic.200800987>.
- Moreno, A., Perez, A., Frigola, J., Nieto-Moreno, V., Rodrigo-Gamiz, M., Martrat, B., Gonzalez-Samperiz, P., Morellon, M., Martín-Puertas, C., Corella, J.P., Belmonte, A., Sancho, C., Cacho, I., Herrera, G., Canals, M., Grimalt, J.O., Jimenez-Espejo, F., Martínez-Ruiz, F., Vegas-Vilarrubia, T., Valero-Garces, B.L., 2012. The Medieval Climate Anomaly in the Iberian Peninsula reconstructed from marine and lake records. *Quat. Sci. Rev.* 43, 16–32.
- Neff, U., Burns, S.J., Mangini, A., Mudelsee, M., Fleitmann, D., Matter, A., 2001. Strong coherence between solar variability and the monsoon in Oman between 9 and 6 kyr ago. *Nature* 411, 290–293.
- Niedermayr, A., Köhler, S.J., Dietzel, M., 2013. Impacts of aqueous carbonate accumulation rate, magnesium and polyaspartic acid on calcium carbonate formation (6–40 °C). *Chem. Geol.* 340, 105–120.
- Olsen, J., Anderson, J.N., Knudsen, M.F., 2012. Variability of the North Atlantic Oscillation over the past 5200 years. *Nat. Geosci.* , <http://dx.doi.org/10.1038/NNGEO1589>.
- Oomori, T., Kaneshima, H., Maezato, Y., Kitano, Y., 1987. Distribution coefficient of Mg<sup>2+</sup> ions between calcite and solution at 10–50 °C. *Mar. Chem.* 20, 327–336.
- Ortega, R., Maire, R., Deves, G., Quinif, Y., 2005. High-resolution mapping of uranium and other trace elements in recrystallized aragonite–calcite speleothems from caves in the Pyrenees (France): Implication for U-series dating. *Earth Planet. Sci. Lett.* 237, 911–923.
- Osborn, T.J., 2011. Winter 2009/2010 temperatures and a record-breaking North Atlantic Oscillation index. *Weather* 66, 19–21.
- Proctor, C.J., Baker, A., Barnes, W.L., 2002. A three thousand year record of North Atlantic climate. *Clim. Dyn.* 19, 449–454.
- Proctor, C.J., Baker, A., Barnes, W.L., Gilmour, R.A., 2000. A thousand year speleothem proxy record of North Atlantic climate from Scotland. *Clim. Dyn.* 16, 815–820.

- Railsback, L.B., Brook, G.A., Chen, J., Kalin, R., Fleisher, C.J., 1994. Environmental controls on the petrology of a late Holocene speleothem from Botswana with annual layers of aragonite and calcite. *J. Sediment. Res. Sect. A Sediment. Petrol. Process.* 64, 147–155.
- Reimer, P.J., Baillie, M.G.L., Bard, E., Bayliss, A., Beck, J.W., Bertrand, C.J.H., Blackwell, P.G., Buck, C.E., Burr, G.S., Cutler, K.B., Damon, P.E., Edwards, R.L., Fairbanks, R.G., Friedrich, M., Guilderson, T.P., Hogg, A.G., Hughen, K.A., Kromer, B., McCormac, G., Manning, S., Ramsey, C.B., Reimer, R.W., Remmele, S., Southon, J.R., Stuiver, M., Talamo, S., Taylor, F.W., van der Plicht, J., Weyhenmeyer, C.E., 2004. IntCal04 terrestrial radiocarbon age calibration, 0–26 cal kyr BP. *Radiocarbon* 46, 1029–1058.
- Scholz, D., Hoffmann, D.L., 2011. StalAge—an algorithm designed for construction of speleothem age models. *Quat. Geochronol.* 6, 369–382.
- Sherwin, C.M., Baldini, J.U.L., 2011. Cave air and hydrological controls on prior calcite precipitation and stalagmite growth rates: implications for palaeoclimate reconstructions using speleothems. *Geochim. Cosmochim. Acta* 75, 3915–3929.
- Sinclair, D.J., Banner, J.L., Taylor, F.W., Partin, J., Jenson, J., Mylroie, J., Goddard, E., Quinn, T., Jocson, J., Miklavič, B., 2012. Magnesium and strontium systematics in tropical speleothems from the Western Pacific. *Chem. Geol.* 294–295, 1–17.
- Spötl, C., Fairchild, I.J., Tooth, A.F., 2005. Cave air control on dripwater geochemistry, Obir Caves (Austria): implications for speleothem deposition in dynamically ventilated caves. *Geochim. Cosmochim. Acta* 69, 2451–2468.
- Spötl, C., Mangini, A., Frank, N., Eichstädter, R., Burns, S.J., 2002. Start of the last interglacial period at 135 ka: evidence from a high Alpine speleothem. *Geology* 30, 815–818.
- Stoll, H.M., Muller, W., Prieto, M., 2012. I-STAL, a model for interpretation of Mg/Ca, Sr/Ca and Ba/Ca variations in speleothems and its forward and inverse application on seasonal to millennial scales. *Geochem. Geophys. Geosyst.* 13, 27.
- Tang, J.W., Dietzel, M., Bohm, F., Kohler, S.J., Eisenhauer, A., 2008. Sr(2+)/Ca(2+) and (44)Ca/(40)Ca fractionation during inorganic calcite formation: II. Ca isotopes. *Geochim. Cosmochim. Acta* 72, 3733–3745.
- Tooth, A.F., Fairchild, I.J., 2003. Soil and karst aquifer hydrological controls on the geochemical evolution of speleothem-forming drip waters, Crag Cave, southwest Ireland. *J. Hydrol.* 273, 51–68.
- Treble, P.C., Chappell, J., Shelley, J.M.G., 2005. Complex speleothem growth processes revealed by trace element mapping and scanning electron microscopy of annual layers. *Geochim. Cosmochim. Acta* 69, 4855–4863.
- Trouet, V., Esper, J., Graham, N.E., Baker, A., Scourse, J.D., Frank, D.C., 2009. Persistent positive North Atlantic Oscillation mode dominated the Medieval climate anomaly. *Science* 324, 78–80.
- van der Schrier, G., Briffa, K.R., Jones, P.D., Osborn, T.J., 2006. Summer moisture variability across Europe. *Journal of Climate* 19, 2818–2834.
- Wang, Y.H., Magnusdottir, G., Stern, H., Tian, X., Yu, Y., 2012. Decadal variability of the NAO: introducing an augmented NAO index. *Geophys. Res. Lett.* 39, 5.
- Wang, Y.J., Cheng, H., Edwards, R.L., Kong, X.G., Shao, X.H., Chen, S.T., Wu, J.Y., Jiang, X.Y., Wang, X.F., An, Z.S., 2008. Millennial- and orbital-scale changes in the East Asian monsoon over the past 224,000 years. *Nature* 451, 1090–1093.
- Wanner, H., Bronnimann, S., Casty, C., Gyalistras, D., Luterbacher, J., Schmutz, C., Stephenson, D.B., Xoplaki, E., 2001. North Atlantic Oscillation—concepts and studies. *Surv. Geophys.* 22, 321–382.
- Ward, N.M., Lamb, P.J., Portis, D.H., El Hamly, M., Sebbari, R., 1999. Climate variability in Northern Africa understanding droughts in the Sahel and Maghreb. In: Navarra, A. (Ed.), *Beyond El Niño: Decadal and Interdecadal Climate Variability*. Springer, Berlin Heidelberg New York, pp. 119–140.
- Wassenburg, J.A., Immenhauser, A., Richter, D.K., Jochum, K.P., Fietzke, J., Deininger, M., Goos, M., Scholz, D., Sabaoui, A., 2012. Climate and cave control on Pleistocene/Holocene calcite-to-aragonite transitions in speleothems from Morocco: elemental and isotopic evidence. *Geochim. Cosmochim. Acta* 92, 23–47.
- Watson, E.B., 2004. A conceptual model for near-surface kinetic controls on the trace-element and stable isotope composition of abiogenic calcite crystals. *Geochim. Cosmochim. Acta* 68, 1473–1488.
- White, W.B., 2004. Paleoclimate records from speleothems in limestone caves. In: Sasowski, I.D., Mylroie, J. (Eds.), *Studies of Cave Sediments Physical and Chemical Records of Paleoclimate*. Kluwer Academic/Plenum Publishers, New York.
- Wong, C.I., Banner, J.L., Musgrove, M., 2011. Seasonal dripwater Mg/Ca and Sr/Ca variations driven by cave ventilation: implications for and modeling of speleothem paleoclimate records. *Geochim. Cosmochim. Acta* 75, 3514–3529.
- Zhang, P.Z., Cheng, H., Edwards, R.L., Chen, F.H., Wang, Y.J., Yang, X.L., Liu, J., Tan, M., Wang, X.F., Liu, J.H., An, C.L., Dai, Z.B., Zhou, J., Zhang, D.Z., Jia, J.H., Jin, L.Y., Johnson, K.R., 2008. A test of climate, sun, and culture relationships from an 1810-year Chinese cave record. *Science* 322, 940–942.
- Zhong, S., Mucci, A., 1989. Calcite and aragonite precipitation from seawater solutions of various salinities: precipitation rates and overgrowth compositions. *Chem. Geol.* 78, 283–299.
- Zuddas, P., Mucci, A., 1998. Kinetics of calcite precipitation from seawater: II. The Influence of the ionic strength. *Geochim. Cosmochim. Acta* 62, 757–766.